

DOE/ER/53192--40

DOE/ER/53192--40

DE90 002543

DESIGN OF THE COMPACT AUBURN TORSATRON*

R.F. Gandy, M.A. Henderson, J.D. Hanson, T. Schneider,

D.G. Swanson

Auburn University

J.R. Cary

University of Colorado

August 1989

Technical Report DOE-ER-53192C-10

DISCLAIMER

This report was prepared as an account of work sponsored by an agency of the United States Government. Neither the United States Government nor any agency thereof, nor any of their employees, makes any warranty, express or implied, or assumes any legal liability or responsibility for the accuracy, completeness, or usefulness of any information, apparatus, product, or process disclosed, or represents that its use would not infringe privately owned rights. Reference herein to any specific commercial product, process, or service by trade name, trademark, manufacturer, or otherwise does not necessarily constitute or imply its endorsement, recommendation, or favoring by the United States Government or any agency thereof. The views and opinions of authors expressed herein do not necessarily state or reflect those of the United States Government or any agency thereof.

MASTER 
DISTRIBUTION OF THIS DOCUMENT IS UNLIMITED

DISCLAIMER

This report was prepared as an account of work sponsored by an agency of the United States Government. Neither the United States Government nor any agency thereof, nor any of their employees, makes any warranty, express or implied, or assumes any legal liability or responsibility for the accuracy, completeness, or usefulness of any information, apparatus, product, or process disclosed, or represents that its use would not infringe privately owned rights. Reference herein to any specific commercial product, process, or service by trade name, trademark, manufacturer, or otherwise does not necessarily constitute or imply its endorsement, recommendation, or favoring by the United States Government or any agency thereof. The views and opinions of authors expressed herein do not necessarily state or reflect those of the United States Government or any agency thereof.

DISCLAIMER

Portions of this document may be illegible in electronic image products. Images are produced from the best available original document.

I. INTRODUCTION

In magnetic fusion research, the class of stellarator toroidal confinement devices (to which the torsatron belongs) are attractive candidates for commercial fusion reactors. Since stellarators do not require plasma current to produce the nested magnetic flux surfaces needed for confinement, they are inherently steady-state devices. Another advantage of stellarators is that they lack the class of current-driven instabilities which may contribute to anomalous transport. Until recently, one drawback of the stellarator class of devices has been the relatively high aspect ratio of the devices when compared to tokamaks. One requires a low-aspect-ratio in order to have an economically feasible toroidal fusion reactor. Historically, the preponderance of high aspect ratio devices came from the natural break-up of the magnetic surfaces as one moved to larger minor radius. Now, with the advent of design optimization techniques such as the one described herein, the design and construction of low-aspect ratio torsatrons has become feasible.

The Compact Auburn Torsatron (CAT) is a low-aspect-ratio torsatron currently under construction at Auburn University and scheduled for completion in December 1989. The machine will replace the Auburn Torsatron ¹ which has been operating since 1984. The design of CAT was done using the Cary-Hanson Optimization technique²⁻⁴. This procedure minimizes the islands which form at rational magnetic surfaces by varying the placement and winding law parameters of the coils. The reduction of the island size effectively increases the plasma volume. In the optimization process the helical field coils are modulated from a straight winding law by the addition of $\alpha_n \sin(n\theta)$ terms, (where θ is the poloidal angle and n is an integer). As well as verifying the Cary-Hanson Optimization technique, CAT will be used to study various magnetic configurations, island sizing and reduction, island effects on the plasma, and the physics of ion cyclotron heating.

The design of CAT is unique among stellarator devices in that it will have two helical field (HF) coils. It will also have the standard set of outer vertical field (VF) coils, and a set of inner VF coils. Two views of CAT are given in Fig. 1. The main component of the HF is provided by the $\ell=2, m=5$ coil which has an aspect ratio $A_C=1.9$. Here ℓ and m refer to the toroidal and poloidal periodicity of the magnetic field, respectively. An additional component of the HF is provided by $\ell=1, m=5$ coil with an aspect ratio $A_C=2.6$. This second coil is needed to keep the magnetic axis circular. One of the constraints on the design of the device was the requirement of using a simple, toroidal vacuum vessel, which also would serve as a coil winding form. This requirement derived from the cost-effectiveness of this approach. With this constraint, any significant 'wobble' of the magnetic axis will cause the outer flux surfaces to collide with the vacuum vessel wall and thus severely reduce the plasma volume. To prevent this from occurring, the $\ell=1$ coil was required. The current in the $\ell=1$ HF coil is opposite that of the $\ell=2$ coil and has the effect of pushing the

magnetic axis toward the vacuum vessel axis. The outer VF coils have a radius of 85 cm and are located at $z = \pm 19$ cm. An inner set of VF coils will also be used in the various configuration studies, the location is currently undecided. All of the coils will be water cooled to provide steady state operation at 1 kG field strength.

The machine is compact with a vacuum vessel aspect ratio $A_v = 3$ and a plasma aspect ratio $A_p \approx 5$. The various parameters of CAT are given in Table I. CAT will have rotational transform ($\tau \equiv 1/q$), $\tau_o \approx 0.3$ on axis, $\tau \approx 0.6$ at the edge, moderate shear, and a magnetic well. Each coil (VF and HF) is designed to allow adjustments to the current centers to optimize the magnetic surfaces. CAT also has the flexibility of adding various helical and toroidal trim coils to further optimize the vacuum magnetic surfaces.

In stellarator construction a great deal of effort is taken in accurately positioning the coils. This effort increases the cost of the device. The previously mentioned trim coils can be used to make adjustments to the current centers and account for small winding errors⁵. Therefore the precision requirements can be relaxed in the building phase of the device. The control of the plasma boundary, which is crucial for impurity control and divertor action, can also be optimized using these trim coils. The CAT vacuum vessel is simple in design and therefore economical. The vessel has a circular cross section and is made of commercially available SS pipe. These design features of CAT, coupled with its relatively low-aspect-ratio, make the machine interesting from a torsatron reactor design perspective.

Much of the work on CAT will be devoted to the study of islands and the related plasma effects. The diagnostics for the island studies (vacuum magnetic surfaces) include the diode and phosphor screen techniques^{1,6} of mapping magnetic surfaces. During plasma operation the diagnostics will include: microwave interferometers, Langmuir probes (1D & 2D), microwave emission, magnetic probes, and visible spectroscopy.

This paper first describes the design and optimization procedure for CAT. Included in this is a description of the Cary-Hanson Optimization technique. In this section the properties of the magnetic fields are presented. Next we present a description of the machine and the construction procedure. Finally the experimental setup for the surface mapping is described and conclusions are presented.

II. DESIGN & OPTIMIZATION PROCEDURE

Recently, considerable effort has been given to the detection of islands that occur at rational surfaces^{7,8} through investigating the vacuum magnetic flux surfaces. Recent work on the Auburn Torsatron⁵ has demonstrated the capability to optimize the magnetic surfaces using trim

coils. This procedure should lead to a corresponding increase in the plasma confinement time and density. The process of minimizing the island size is uncertain. One purpose of CAT is to provide a test-bed for the reduction of magnetic islands through modifications in the magnetic configuration using trim coils. This investigation requires a significant amount of machine time devoted to vacuum surface mapping. This would be impractical on larger machines, where plasma operation is the main goal. However a small research device such as CAT is ideally suited to thoroughly investigate an important reactor issue such as this.

The general design goal of CAT was to design a low-aspect-ratio torsatron. The Cary-Hanson optimization technique was used to accomplish this goal. The pre-conditions of the design were : (1) design a $\ell=2$ torsatron, (2) keep the m number as low as possible to maximize access, (3) have moderate shear with $\tau_0 \approx 0.3$, (4) have a near circular magnetic axis, and (5) have an plasma aspect ratio ≤ 5 . Since the CAT research program focuses on magnetic island studies, care was taken to insure that the rotational transform profile had as many relevant rational surfaces as possible. Another constraint on the machine design was to insure the presence of the $\tau = 1/2$ surface in the rotational transform profile. The $\tau = 1/2$ surface, being a low order rational surface, will characteristically display a large island compared to most other rational surfaces, since island size typically decreases as order number increases.

The Cary-Hanson optimization technique²⁻⁴ was used to design the machine. The technique minimizes the stochasticity of the field line flow and thereby maximizes the enclosed plasma volume. This process calculates the residuals associated with selected rational field lines. The magnitude of the residuals of a rational are directly related to the size of the magnetic island formed at that particular rational. The magnetic field modeling was done with the Integrable Field Stellarator (IFS) code³. The coils are represented as a collection of connected straight line filaments. The filament endpoints lie on a continuous curve called the winding law. A convenient parameterization for the helical coil winding law is

$$\phi = \frac{\ell\theta}{m} \pm \sum \alpha_n \sin(n\theta)$$

where $\phi(\theta)$ is the toroidal (poloidal) angle, and the \pm refer to the two components of the main helical coil.

Several configurations were investigated to yield the optimal machine. Examples of designs investigated include : (1) $\ell=2$, $m=6$ designs with and without toroidal field coils; (2) $\ell=2$, $m=5$ designs with and without toroidal field coils; (3) $\ell=2$, $m=6$ design with helically scalloped VF coils; and (4) $\ell=2$, $m=5$ designs with an $\ell=1$, $m=5$ auxiliary HF coil. In most cases the configurations failed to yield an acceptable rotational transform or aspect ratio, or had excessive wobble of the magnetic axis. Ultimately the $\ell=2$, $m=5$ torsatron with an inner $\ell=1$, $m=5$ minor coil was chosen as the best candidate in view of construction limitations and machine parameters.

The parameters of the machine were systematically modified to minimize chaotic field lines, yet keep the rotational transform on axis at the required value. The list of parameters includes the currents in each coil, coil aspect ratios, coil locations, the α_1 term of the $\ell=1$ coil, and the $\alpha_1, \alpha_2, \alpha_3$ terms of the $\ell=2$ coil (all other α_n values were set = 0). The procedure also kept the magnetic axis locked to the vacuum vessel axis (within 2 mm) at every field period and also at every half field period.

Up until this point in the design process the code considered each coil as a single filament. When the optimized single filament design was converted to a realistic multi-filament situation, the overall shape of the flux surfaces changed very little, but the rotational transform dropped dramatically (see Figure 2). In modeling the finite coils more filaments were added until there was no significant change in the surface of section or the rotational transform from the previous number of filaments. Due to the low-aspect-ratio of CAT several filaments per helical coil (typically 16) were required to closely model the real coil situation.

It was noted that the major factor in decreasing the transform was the large cross-section of the $\ell=2$ coil pack. At this point in the design the aspect ratio of both coils were established preventing any modification to the coil pack cross-sectional dimensions. Therefore, to increase the rotational transform, we re-optimized (in multi-filament mode) using the α_n 's of both the helical coils as parameters. The final winding law obtained for the $\ell=2$ coil is:

$$\phi = \frac{2\theta}{5} - 0.21 \sin(\theta) + 0.04 \sin(2\theta) - 0.02 \sin(3\theta)$$

and for the $\ell=1$ coil:

$$\phi = \frac{\theta}{5} - 0.1 \sin(\theta)$$

The resultant rotational transform profile for the final design is shown in Figure 3. Plots of two surface-of-sections are shown in Figures 4 & 5.

III. MACHINE DESIGN

A. Vacuum Vessel

The vacuum vessel for CAT was designed to be approximately the same size as the existing Auburn Torsatron. A simple design was chosen to minimize machining costs. As mentioned earlier, the major part of the vacuum vessel is formed by welding four 90° bends together to form the torus. The wall thickness of the bends are 0.48 cm and made of 306 stainless steel. The tolerances on the machining of the torus are somewhat relaxed to further reduce costs, ± 0.48 cm over the 53.3 cm major diameter. A layer of epoxy on the vacuum vessel is used to form the actual winding surface for the coil pack. The width of the epoxy is ~ 1.0 cm. This allows 0.5 cm

tolerance on both the major and minor radius of the torus and still preserve the capability of forming the correct size toroidal surface with epoxy.

The port location and size was chosen to maximize access and also utilize many existing vacuum components from the current Auburn Torsatron. The vertical port extensions and flanges on CAT were modeled after the side port extensions and flanges on the Auburn Torsatron. These are ASA type flanges for the 20 cm diameter ports. The vertical ports had to be toroidally shifted from an up/down symmetric position to fit between the helical coils (see Figure 1B). The optimum shift was determined by centering the port between the helical coils. The ports are shifted $\pm 13^\circ$ at the beginning of each field period (+, - refers to the direction of the toroidal shift for the bottom, top ports respectively). The magnitude of the shift unfortunately prohibits any up/down port overlap which would be convenient for microwave interferometry.

The horizontal ports were designed with a square cross section. This shape allows adequate access while still maintaining a fairly simple machine design. The optimum size of the port was 30 x 30 cm. This specific port size permits a circular screen having the diameter of the vacuum vessel cross section to be passed through the port. This proves convenient for the extensive surface mapping to be performed on CAT. In summary, the low-aspect-ratio feature of CAT allows for good access for plasma diagnostic and heating applications.

B. Description of Winding Jigs

As previously mentioned, epoxy is placed on the vacuum vessel to define the toroidal surface which the coils will rest on. The purpose of the epoxy is two fold. First, the epoxy provides an extra insulation break between the coils and the vacuum vessel. Second, the epoxy can be shaped and sanded to form a near perfect toroidal surface. This relaxes the machining precision requirements on the torus. The epoxy was chosen for its pliability while curing, machineability, strength and insulation properties. Five different epoxies were tested for suitability and the epoxy of preference was 3-M Electrical Resin (Product # 10). The epoxy is placed on the vacuum vessel (~1cm thick) and sanded to obtain a near toroidal surface (within 1 mm).

The toroidicity of the epoxy layer is checked using a device called the epoxy jig, see Figure 6. The rotary arm of the epoxy jig is mounted on a 25.4 cm rotary table which provides 360° of toroidal rotation. A steel bar extends upward along the central axis of the vacuum vessel. At the end of this bar is an aluminum plate running radially outward which has two other plates extending down from it, one on the inside of the torus, the other on the outside. These plates are mounted on rotary unislides which permit the correct positioning of the plates radially (major radius) in and out from the axis of the torus. Each unislide has 38 cm of travel to position the plates for the $\ell=1$ and $\ell=2$ coils as well as to clear the horizontal port as the jig rotates through 360° in the toroidal direction. Attached to the vertical plates are various templates which are used to check the toroidicity of the epoxy. Several templates have been made to reach all locations under both the

$\ell=1$ and $\ell=2$ coils. The templates have marks located every 10° poloidally along their arcs so that once the epoxy has been shaped correctly, the coil locations can be marked. The jig is removed each time a helical coil set is wound.

An adjustable support table was built to provide accurate placement of the jig. The table has 5 degrees of freedom to insure the jig is placed coaxially with the machine and at the right height. The table consists of three plates. Two plates allow adjustments in the horizontal plane. The third plate is supported by three threaded rods to raise or lower the epoxy jig and adjust the jig to be coaxial with the torus.

C. Helical Winding Jigs

Once the epoxy has been shaped and the location of a given coil has been identified on the surface of the epoxy, the vacuum vessel is ready for coil winding. The wire that is wound on CAT is made of soft tempered copper with a dimensions of $0.89\text{ cm} \times 0.89\text{ cm}$, and a 0.02 cm coating of Dacron glass insulation. This copper wire has a 0.64 cm diameter hole running along its length. This allows water cooling of the coil pack and steady state operation with a 1.0 kG field (500 Amperes of HF coil current). The cross sectional size of the conductor was determined by the existing power supplies (two 180 Volt, 200 Ampere, DC supplies). Since the length of the CAT coils is similar to the length for the existing Auburn Torsatron, the cross section of the copper was kept approximately the same. To wind the wire it is first placed on a winding spool. The spool encircles the poloidal axis of the vacuum vessel. About 45 kg (≈ 50 meters) of wire is loaded onto the spool. The wire is unwrapped from the spool as the spool moves toroidally around the vacuum vessel. Removable jacks support the vacuum vessel during the winding process. A jack is placed at each bottom port. Each time the winding spool is advanced, a jack is replaced. As the wire is fed from the spool, it is clamped in place using mounting clamps. The clamp preserves the integrity of the coil pack while additional turns are being added. The clamps are bolted to the vacuum vessel by studs welded to the surface of the vacuum vessel which are located at 45° poloidal increments with the first clamp at $\theta=0^\circ$ (outside mid-plane). During the process of wrapping a coil, the clamp is removed and the wire is positioned. Once the final turn is wound, the clamps are replaced with permanent fixtures to hold the pack together.

The $\ell=1$ helical coil is wound first and is supported by epoxy on the vacuum vessel. The $\ell=2$ coil is wound next outside of the $\ell=1$ coil. The $\ell=2$ coil is supported by a bridge made of copper sheets and epoxy. The bridge is held in place by standoffs from the vacuum vessel or rests directly on the $\ell=1$ coil pack. The standoffs are again attached by studs welded directly to the vacuum vessel. The copper sheets are mounted onto the standoffs and form rigid surfaces on which to apply the epoxy. The epoxy is then shaped to provide a toroidal winding surface for the $\ell=2$ coil. During this process the winding jig is again inserted to measure the toroidicity of the epoxy as well as to mark the $\ell=2$ coil location. The mounting clamp design is modified from the

$\ell=1$ clamps since the $\ell=2$ coil is not directly supported from the vacuum vessel. Again, the clamps are located around the machine at 45° poloidal increments due to the location of the $\ell=1$ coil beneath the $\ell=2$ coil. To account for this, temporary supports are placed at various poloidal locations to keep the wires from slipping off their designated path.

Since a hollow conductor is being used, steps are taken to insure an electrically sound connection which does not impede water flow each time the wire sections are spliced. The ends of the two wires that are to be spliced together are first stripped of their insulation, and then placed in a splicing jig, where the hole is enlarged by drilling out each end, then the copper is cut to a 30° angle. A small copper tube, which has the same inner diameter as the wire, is placed in the drilled out region. Next the two wires are silver soldered together. The weld is checked by flow tests to insure the hole is not clogged. The region where the weld is made is sanded and recoated with kapton tape.

Periodically there are electrical breaks and coolant breaks in the helical windings. The break requires a special adaptor to allow both electrical and coolant feeds. This adaptor is made from a piece of the conductor that is bent in an arc to redirect the coolant flow without significantly adding turbulence to the flow. The feeds are spliced into the end of the wire as described above.

D. Coil Pack Description

Each of the helical coil packs has four electrical breaks built into them. The breaks will separate each pack into four layers, see Figure 7. By changing the current ratios in each of the four layers, the effective aspect ratio of the current center can be altered. At 0.5 kG (half-field operation), the aspect ratio the $\ell=1$ coil pack of the can be adjusted from 0.37 to 0.41, and the $\ell=2$ aspect ratio can be adjusted from 0.48 to 0.55. This flexibility, coupled with a $\ell=2 \sin\theta$ trim coil, can effectively adjust the current centers of the helical coil so as to alter the winding law of CAT. Adjustments to the winding law could prove useful in optimizing the machine after it has been constructed in order to induce and remove magnetic islands.

An $\ell=2, \sin\theta$ trim coil will ride outside of the $\ell=2$ coil. The trim coil will consist of two separate coilpacks. The winding laws of the two packs are given by:

$$\phi_1 = \phi_m - \alpha_t \sin(\theta)$$

and $\phi_2 = \phi_m + \alpha_t \sin(\theta)$

where ϕ_m is the main $\ell=2$ winding law and α_t is the $\ell=2, \sin\theta$ trim coil constant (approximately 0.1). Note that $\alpha_t \sin(\theta)$ is added to one winding law and subtracted from the other winding law.

The same magnitude of current will run in both coil packs but in opposite directions. By running the current in opposite directions a net $2\alpha_t \sin(\theta)$ term is added to the $\ell=2$ current center winding

law without changing the $\ell=2$ coil, net aspect ratio. This allows one to independently modify the average coil aspect ratio and trim coil effects.

Like the helical coils, the VF coils also are broken up into sections. The pack is broken up into five sections radially and an additional two sections are added in the vertical direction, see Figure 8. The radial sections allow for adjustment in major radius of the VF current center by altering the current ratio in each section. Operating CAT at 1kG (full field), the radius of the VF coil current center can be adjusted ± 1.9 cm. The additional division vertically can raise or lower the current center by ± 2.9 cm. The mechanical support of the VF coils will allow the coils to be tilted and shifted. This flexibility will allow further investigation of the effects of islands due to errors in the VF coil placement.

The exact positions of the inner VF coils are not yet determined. The coils will be positioned to provide the maximum flexibility in adjusting the rotational transform, which will be determined by using the Cary-Hanson optimization technique. The inner VF coils will be powered separately to allow a quadrupole configuration on all the VF coils. Again, the inner VF coil will be used in magnetic configuration studies of magnetic islands.

E. Support Structure

The support structure for CAT is designed mainly to support the machine from loads due to gravity as the magnetic forces are small compared to gravitational forces. Since the machine has a five-fold symmetry, the support structure consists of five supports toroidally located between the bottom vertical port and the $\ell=2$ helical winding. Insulating material is cut to match the contour of the vacuum vessel and is bolted to the vessel using L-brackets. On the other end the insulating pieces are straddled by an aluminum standoffs. The machine can be leveled by placing shims underneath the insulating pieces, with the weight of the machine (approximately 2,000 pounds) holding the shims in place. The standoffs rest on aluminum bars which run radially underneath the vacuum vessel, these bars also support the VF coils. Note shims are also used to level the VF coils. From each of the five aluminum bars, there are two aluminum tubes which extend to the floor. These 7.6 cm diameter tubes are bolted to the floor. This design provides ample room to access the bottom ports while still providing stable support for the machine and VF coils. Furthermore, the VF coil supports are designed to allow the desired shifts and tilts of the coils for island studies due to various VF coil location perturbations.

IV. SURFACE MAPPING SETUP

The research emphasis of CAT will be magnetic island studies. Therefore, extensive work will be done in the field of vacuum magnetic surface mapping. The experimental setup for the surface mapping is modeled after previous experiments ^{1,6}. The phosphor screen technique ^{6,9} will be the primary method of magnetic surface mapping. To a lesser extent the diode technique ^{1,10} of surface mapping will be used. With the phosphor screen method a high transparency screen is coated with sodium salicylate. The sodium salicylate is applied by dissolving it in ethyl alcohol then spraying on the screen with an atomizer. Typically, 5-10 coatings are applied. The screen is then placed in a poloidal plane of the machine. A CCD camera is placed on a horizontal plane with a view of the screen. An electron beam gun is placed on the opposite side of the machine. The gun is mounted on a probe with two degrees of freedom. The probe allows the positioning of the gun anywhere in the poloidal cross section. Our particular probe has been used for surface mapping on the Auburn Torsatron¹ and has been adapted for use on CAT. A view of the setup can be seen in Figure 9.

The resulting image formed by the electron beam interacting with the phosphor screen is read from the CCD camera and recorded on a ED-Beta VCR. The VCR provides high resolution (500 horizontal lines) and insures no degradation in the picture quality. Lower resolution VCRs (such as standard VHS recorders) tend to diminish the contrast of the picture. The recorded image from the VCR is displayed on an Apple Macintosh II using an image capture board (Scion Image Capture 2). The image then can be analyzed to determine volume, island size, rotational transform, etc. Software has been written to remove distortion and enhance the image. The sources of distortion include : (1) non-normal viewing angle, (2) camera lens distortion, (3) image capture distortion, and (4) computer monitor display distortion. The overall distortion was measured by viewing a calibration grid with the CCD camera. The distortion of the calibration grid was measured and recorded. The transformation used to remove the distortion from the calibration grid is then used in subsequent surface mapping with the phosphor screen technique.

V. Conclusions

We have presented details of the design of a low-aspect-ratio torsatron, an attractive candidate for a future fusion reactor. The attractive features of low-aspect-ratio torsatrons include: plasma current free operation, good diagnostic and heating access, and flexible magnetic configuration. The first use of the Cary-Hanson optimization technique to design a machine has

been demonstrated. CAT will have trim coils to allow detailed studies of the important question of magnetic islands.

ACKNOWLEDGEMENTS

The authors would like to thank David Bluestein, Ron Gilchrist, Steve Knowlton and Kevin Ross of Auburn University for valuable assistance. We also thank Jeff Harris of Oak Ridge National Laboratory for support and encouragement. This work was supported under U.S. Department of Energy grant DEFG605-85ER53192C. Jim Hanson was also supported by the United States National Science Foundation, grant NSF-PHY-8451275 with matching grants from Maxwell Laboratories, Inc., TRW Corporation, and Allied Signal Corporation. John Cary was also supported by U.S. Department of Energy grant DEFG02-85ER53207.

REFERENCES

1. Gandy, Henderson, Hanson, Hartwell, and Swanson; "Magnetic Surface Mapping with an Emissive Filament Technique on the Auburn Torsatron", *Review of Scientific Instruments*, **58** (4), p. 509, April 1987.
2. Hanson and Cary, " Elimination of Stochastisity in Stellarators", *Phys. of Fluids*, **27** (4), p. 767, Apr. 1984.
3. Cary and Hanson, " Stochastisity Reduction", *Phys. of Fluids*, **29** (8), p. 2464, Aug. 1986.
4. Cary, *Phys. Rev. Letts.*, "Vacuum Magnetic Fields with Dense Flux Surfaces", **49** (4), p. 276, 1982.
5. Henderson, Gandy, Hanson, Hartwell, and Swanson; " Magnetic Surface Optimization on the Auburn Torsatron", *Nuclear Fusion*, Volume 28, No.6, (1988).
6. Hartwell, Gandy, Henderson, Hanson, and Swanson; "Magnetic Surface Mapping with Highly Transparent Screens on the Auburn Torsatron", *Review of Scientific Instruments*, **59** (3), p. 460, March 1988.
7. Hailer, Massig, Schuler, Schoworer and Zwicker, "Studies of the Magnetic Surfaces in the Stellarator Wega"; *Proc. of the 14th Eur. Conf. on Contrl. Fusion and Plasma Physics*, June 1987.
8. Colchin, Anderson, England, Gandy, Harris, Henderson, Hillis, Kindsfather, Lee, Million, Murakami, Neilson, Saltmarsh and Simpson; "Electron Beam and Magnetic Field Mapping Techniques Used to Determine Field Errors in the ATF Torsatron", *Review of Scientific Instruments*, August 1989.
9. A. V. Georgievskij, Y. V. Gutarev, A. G. Dikij *et al.*, "Proceedings of the 12th European Conference on Controlled Fusion and Plasma Physics," supplement to *Proceedings of the 12th European Conference on Plasma Physics and Controlled Nuclear Fusion Research*, Budapest, Vol. 9F, Part 1 (1985).
10. R. Takahashi, et al., "Measurements of Magnetic Surfaces on Heliotron-E", in *Proc. of Int. Stellarator/Heliotron Workshop, IAEA Tech. Comm. Meeting*, Vol.II, p.220, (1986).

FIGURE CAPTIONS

Figure 1A. Top view of CAT.

Figure 1B. Side view of CAT.

Figure 2. Rotational transform versus major radius for optimized single filament design (open circles) and for the same winding law in the multi-filament case (closed circles). Note the dramatic drop in rotational transform when the coils are modeled as multi-filaments.

Figure 3. Rotational transform versus major radius for final, optimized, multi-filament design.

Figure 4. Surface-of-section for final design at $\phi=0^\circ$. The coordinates are defined as follows : $X=R/R_o$ and $Y=z/R_o$ where z is defined as the vertical dimension and R is the major radius. ($R_o=53.3$ cm).

Figure 5. Surface-of-section for final design at $\phi=36^\circ$ (1/2 field period from Figure 4 case) . The coordinates are defined as follows : $X=R/R_o$ and $Y=z/R_o$ where z is defined as the vertical dimension and R is the major radius. ($R_o=53.3$ cm).

Figure 6. Schematic of epoxy winding jig. This jig allows measurement in three dimensions (major radius R , toroidal angle ϕ , and poloidal angle θ) to a linear accuracy of less than 1 mm.

Figure 7. Cross sectional view of the HF coil packs.

Figure 8. Cross sectional view of the VF coil packs.

Figure 9. Schematic of the phosphor screen surface mapping experimental set-up.

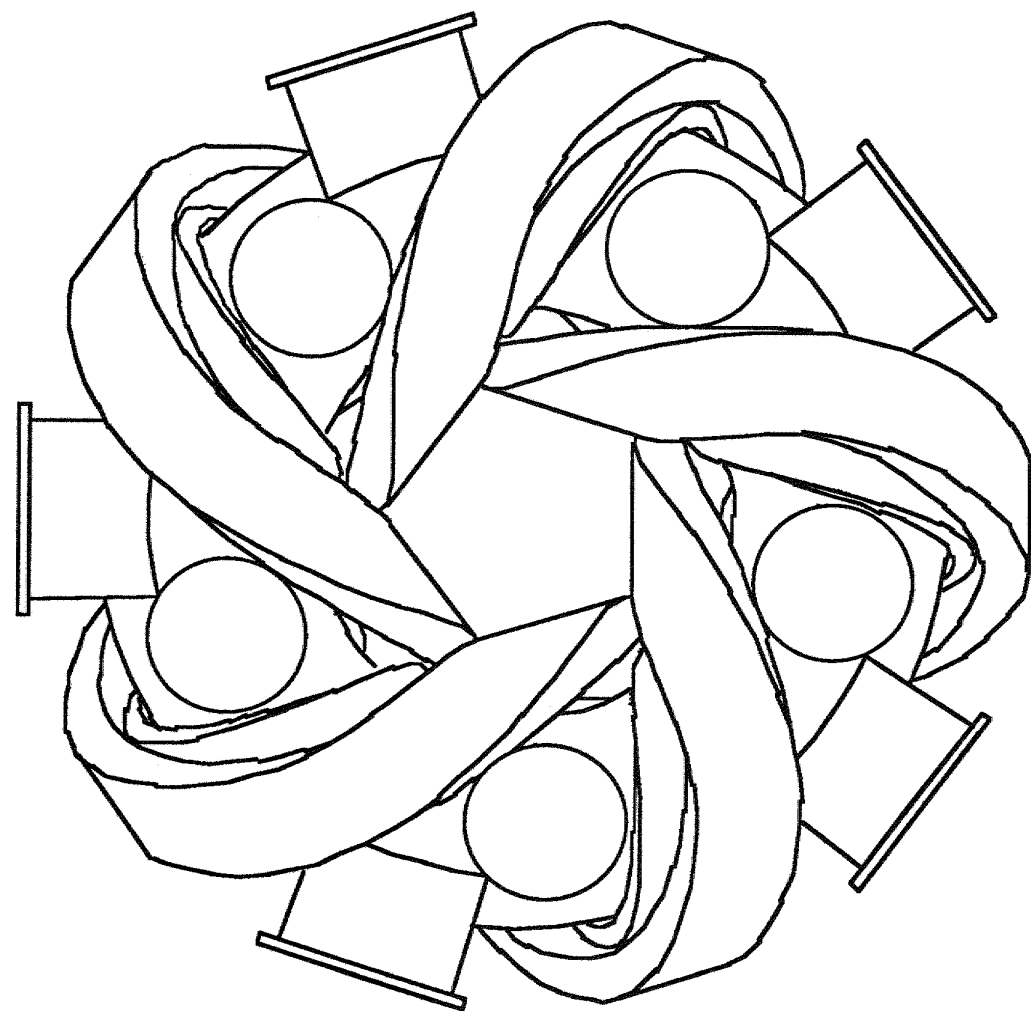


Figure 1A

DESIGN OF THE COMPACT AUBURN TORSATRON

Gandy et al.

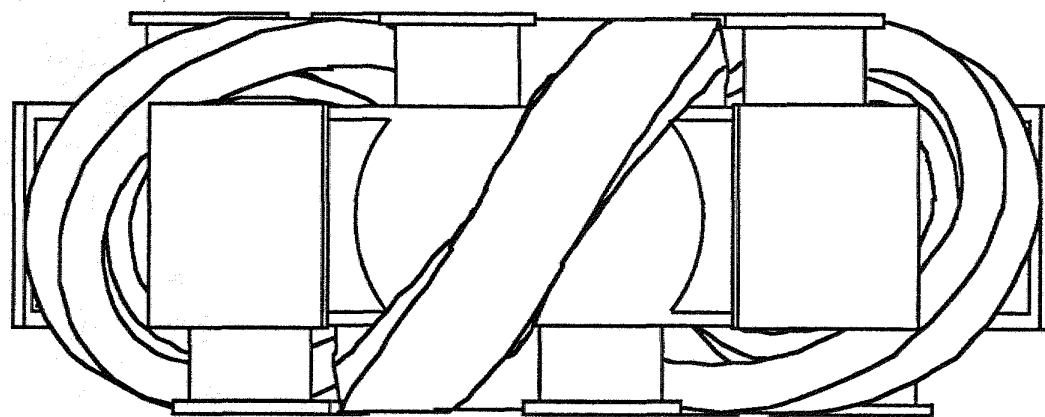


Figure 1B

DESIGN OF THE COMPACT AUBURN TORSATRON

Gandy et al.

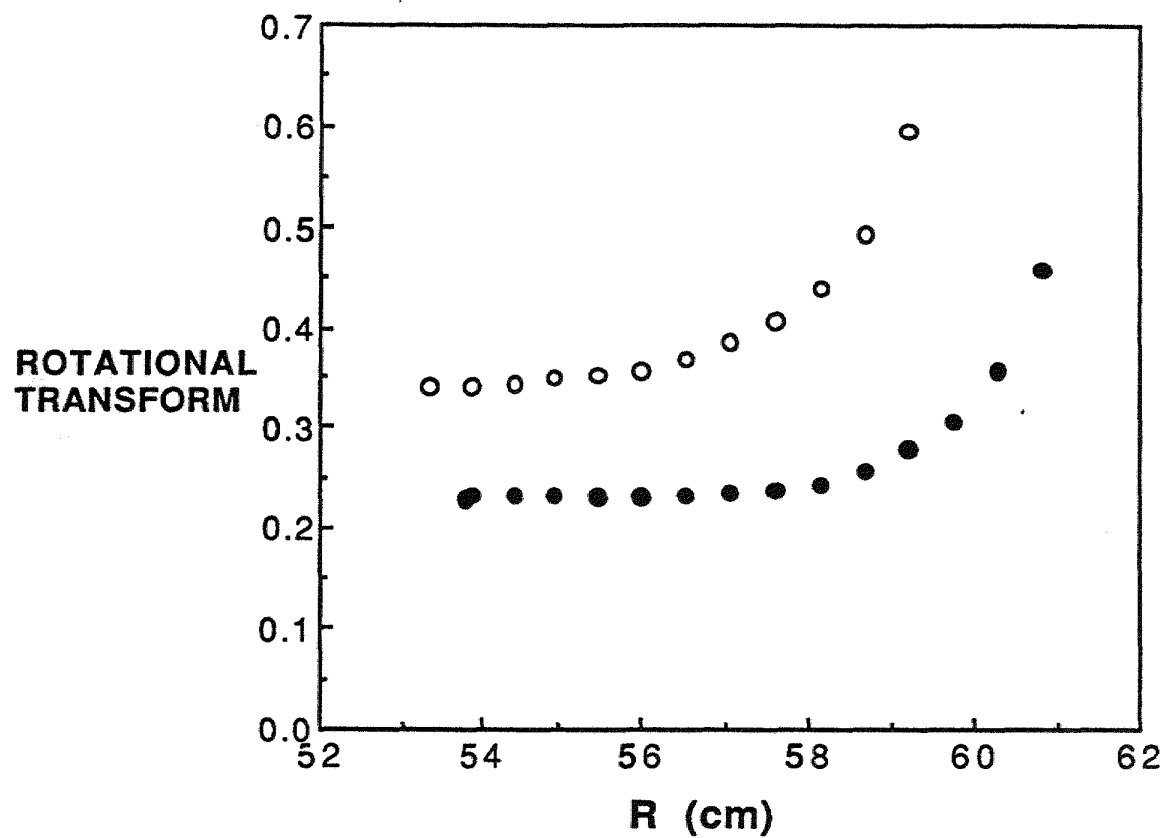


Figure 2

DESIGN OF THE COMPACT AUBURN TORSATRON

Gandy et al.

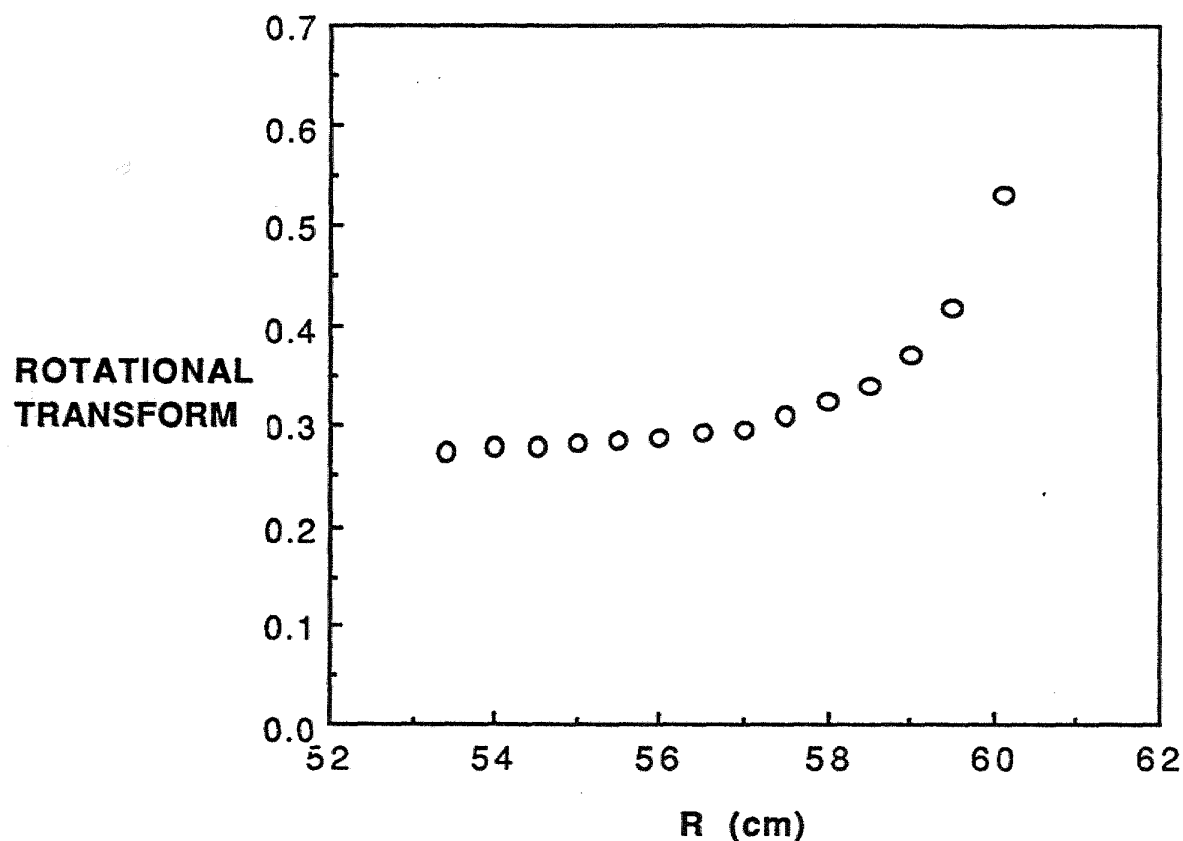


FIGURE 3

DESIGN OF THE COMPACT AUBURN TORSATRON

Gandy et al.

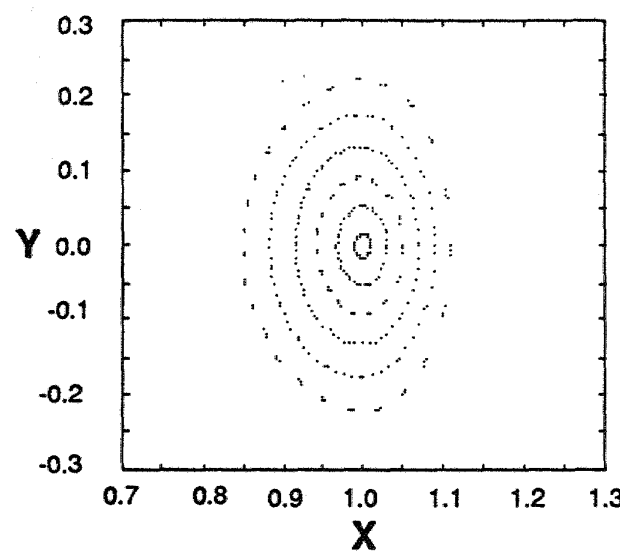


FIGURE 4

DESIGN OF THE COMPACT AUBURN TORSATRON

Gandy et al.

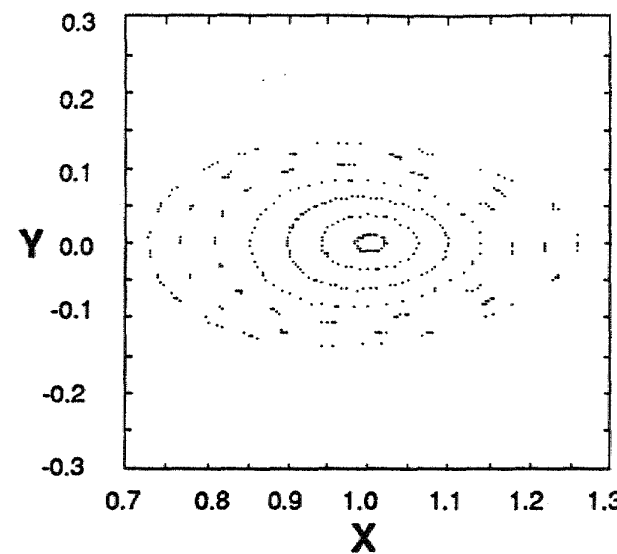


FIGURE 5

DESIGN OF THE COMPACT AUBURN TORSATRON

Gandy et al.

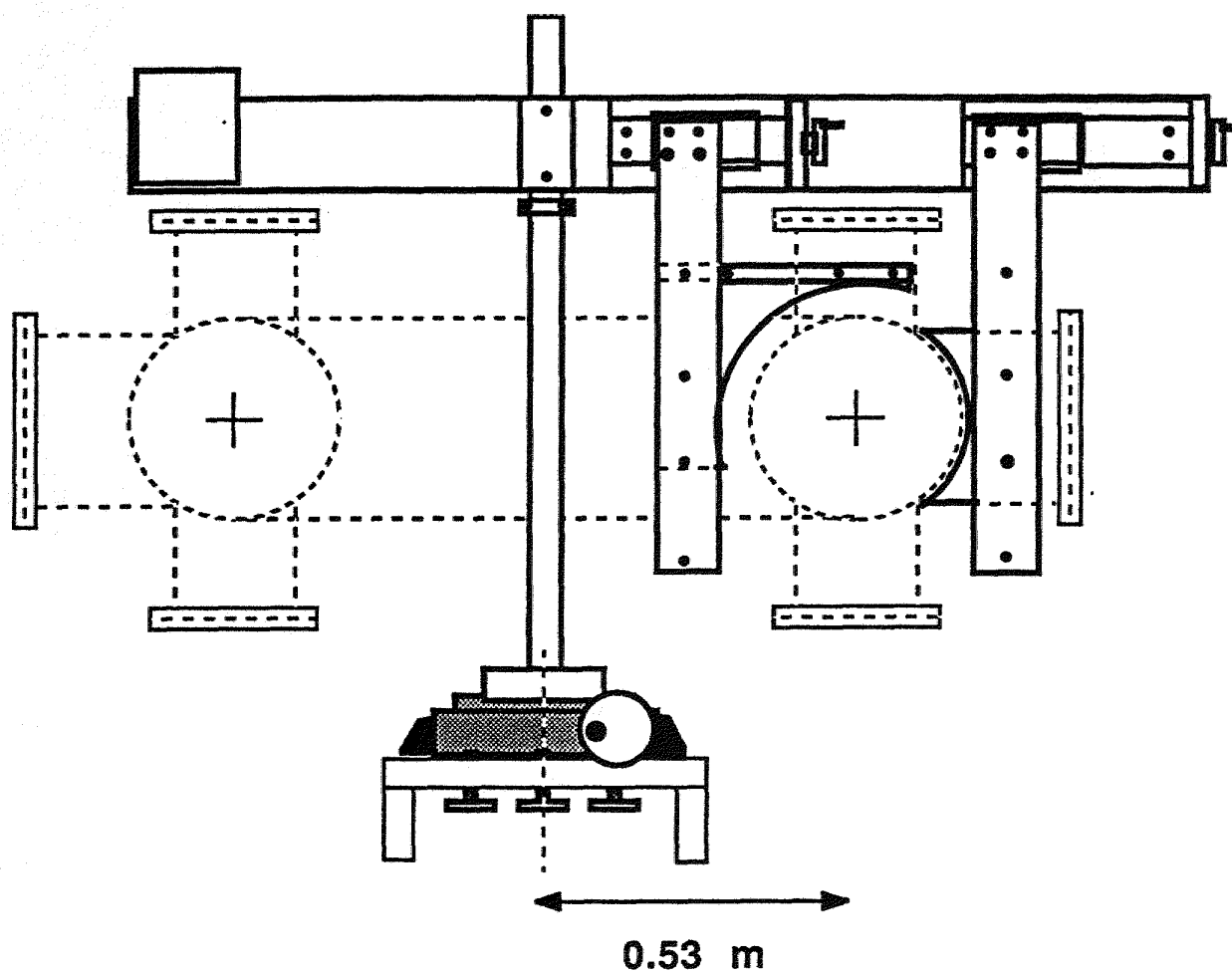


Figure 6

DESIGN OF THE COMPACT AUBURN TORSATRON

Gandy et al.

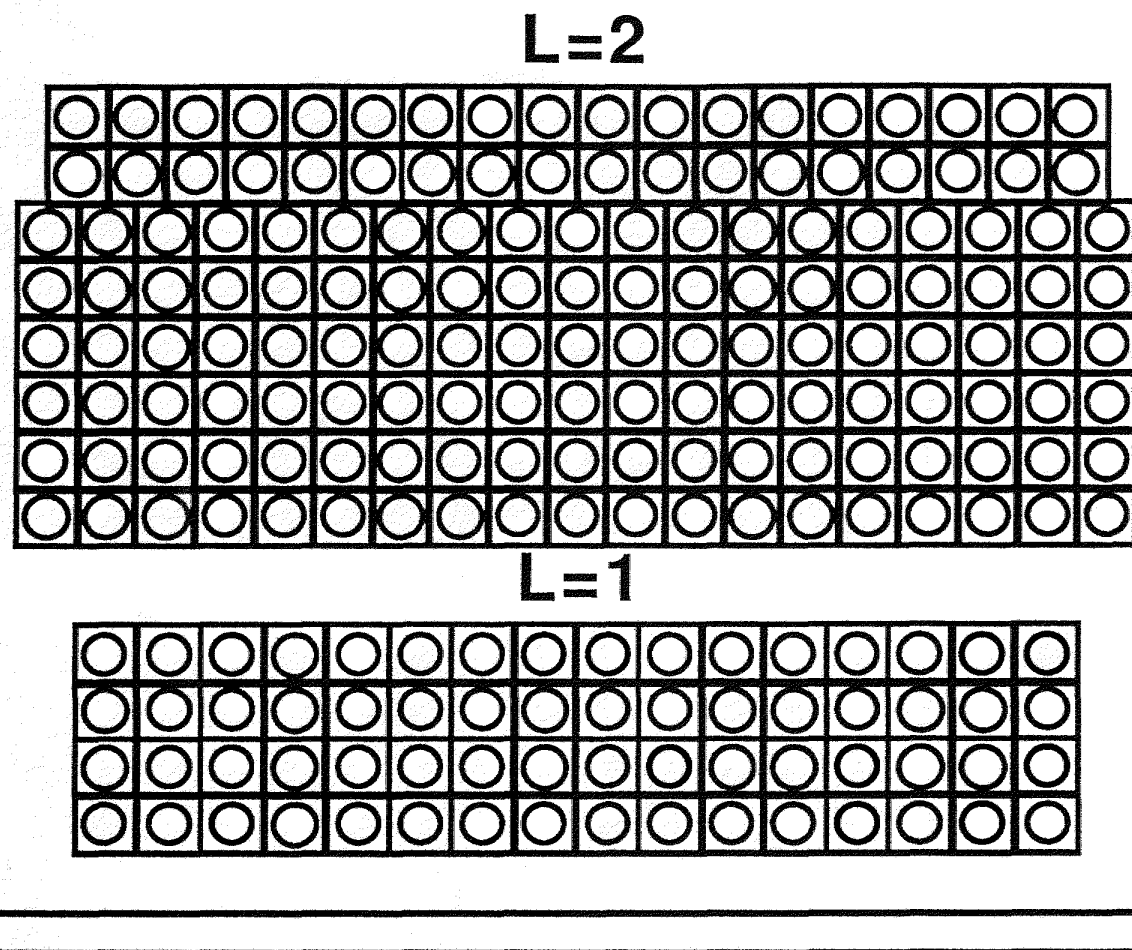


Figure 7

DESIGN OF THE COMPACT AUBURN TORSATRON

Gandy et al.

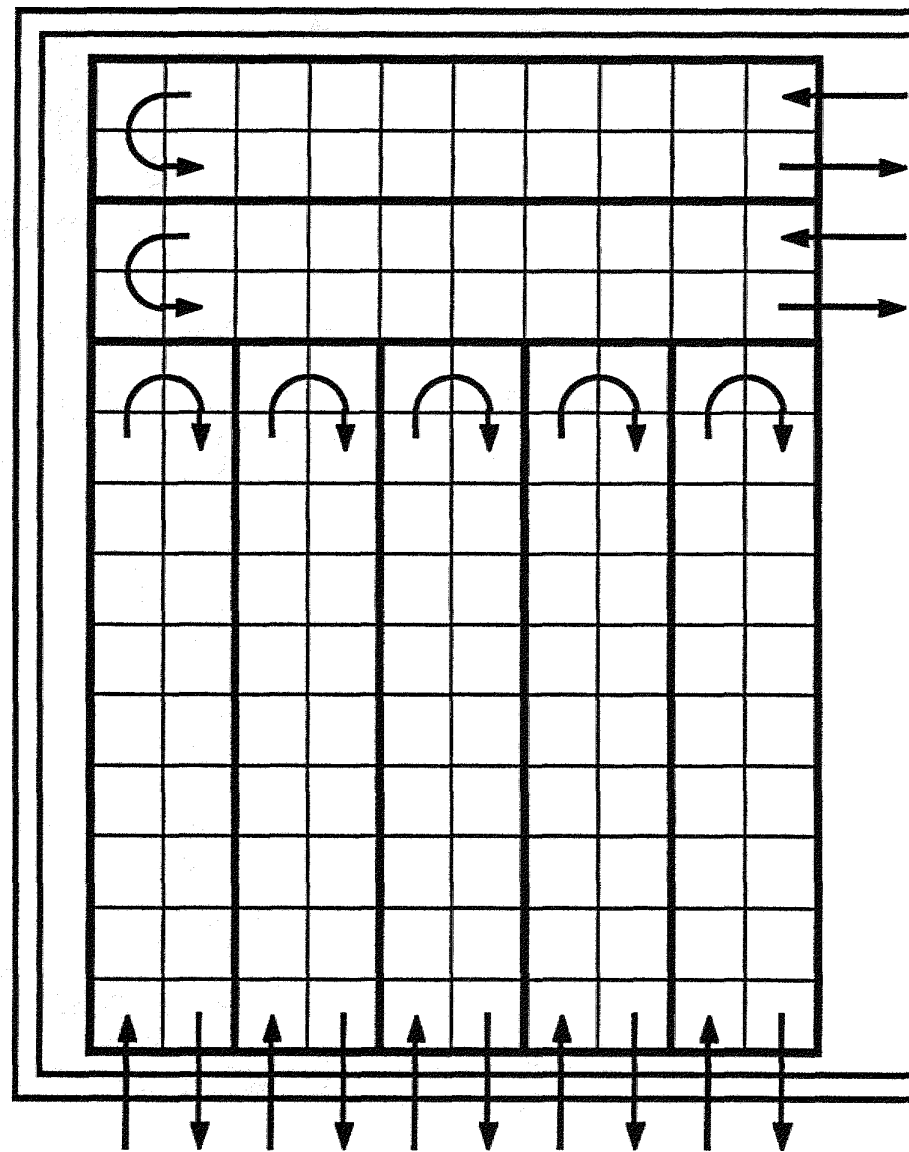


FIGURE 8

DESIGN OF THE COMPACT AUBURN TORSATRON

Gandy et al.

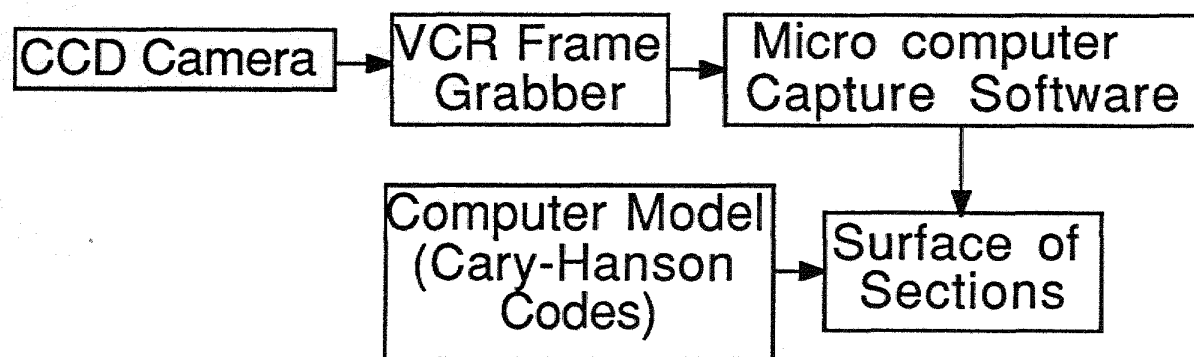
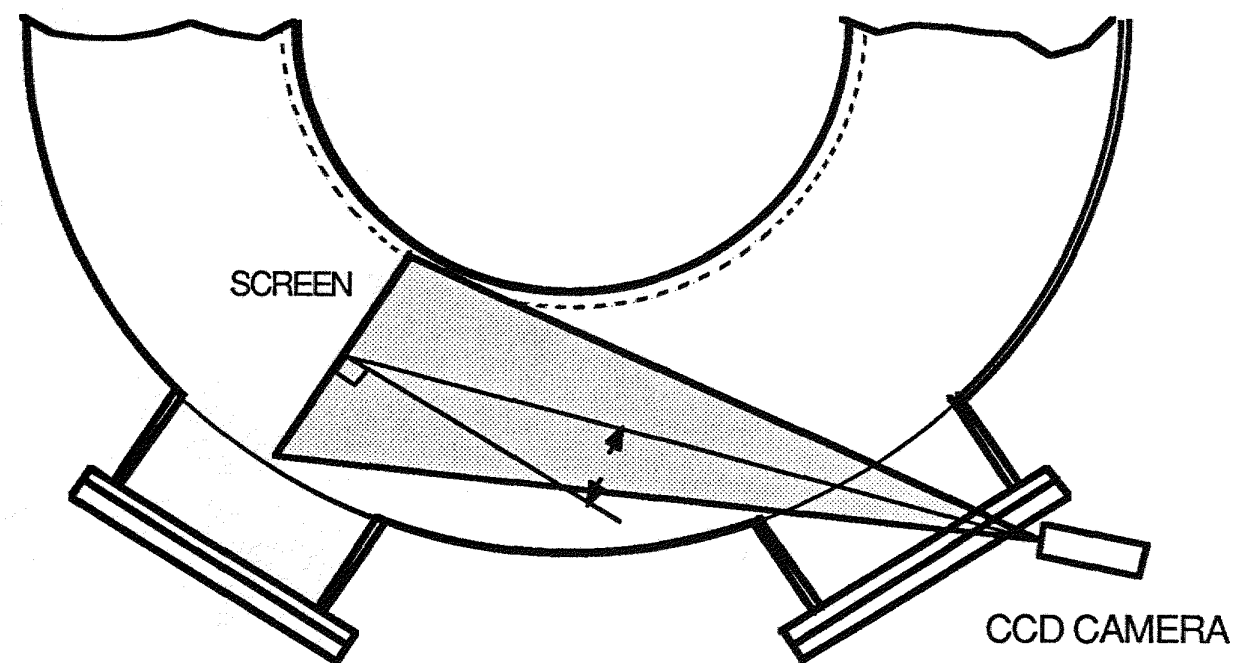


Figure 9
DESIGN OF THE COMPACT AUBURN TORSATRON

Gandy et al.

Table I. CAT PARAMETERS

Major Radius	53.3 cm
Avg. Minor Radius	11 cm
Vacuum Vessel Rad.	16.8 cm
Avg. Hel. Coil Rad.	
l=2	27.4 cm
l=1	20.6 cm
Number of Turns	
l=2 Coil	150
l=1 Coil	60
VF per	60
Multipole Order	2 (1)
No. of Field Periods	5
Rotational Transform	
$\tau(0) \approx 0.3$	
$\tau(\text{edge}) \approx 0.7$	
Magnetic Field, B_0	1 kG
Main Coil Set	177V/500A(2) DC
ECH Power	1 kW CW @ 2.45 GHz
ICH Power	5 kW CW @ 1-30 MHz
	50 kW Pulsed